Using Peak Season NDVI for Assessing Soil Constraints Under Different Climate Conditions

Fathiyya Ulfa(✉), Thomas G. Orton, Yash P. Dang, and Neal W. Menzies

School of Agriculture and Food Sciences, The University of Queensland, St. Lucia, QLD 4072, Australia
f.ulfa@uqconnect.edu.au

Abstract. Impacts of soil constraints limiting yields often depends on climate. In years with adequate rainfall, only small impacts of soil constraints are expected. But in dry years, soil constraints can limit plant water uptake and trigger spatial variation in crop growth. In wet years, waterlogging-related constraints can play an important role in the spatial variation of crop growth. We used remote sensing data in Australia's Northern grain-growing region (from Landsat, average NDVI over periods of high biomass) to investigate the relationship between climate and constraints. The correlations between constraints and the average NDVI in different rainfall years were analyzed. The results showed that the average NDVI was most significantly correlated with constraints in wet years. Possible explanations are that waterlogging associated with sodicity severely affected plant growth in wet years or that the imagery or rainfall data used were not representative of soil constraint impacts and their dependence on climate.

Keywords: NDVI · Soil Constraints · Climate

1 Introduction

Soil constraints can have a major impact on crop yield. In northern grains-growing regions of Australia, the most influential constraints are the constraints related to salt content [1, 2], which might link to soil water stored from rainfall and ability of roots to access stored water [3–6]. Thus, a portion of yield variation might be best explained by the combined effect of both soil constraints and rainfall.

Rainfall is the major driver of the temporal variation of soil water, controlling crop growth and productivity [2, 6]. Spatially, across a field, plant-available soil water (PAW) is controlled by the soil's capacity to store water [6] and is impacted by certain soil constraints, which can affect the plant's ability to extract water from the soil for growth.

The impact of soil constraints on PAW and yield is dependent on climate, in a very dry season the plant is more reliant on access to stored soil moisture and the presence of soil constraints that restrict either the storage of soil water, or the ability of the crop to take up soil water, are likely to reduce yield. So, we might expect correlations between soil constraints (which limit the storage and the plant extraction of soil water) and crop growth to be strongest in very dry growing seasons. In a very wet growing season with

J. Sumantyo et al. (Eds.): ICoSIA 2022, ABSR 29, pp. 464–476, 2023.
https://doi.org/10.2991/978-94-6463-122-7_44

intense rainfall events, we might expect soil constraints that reduce soil drainage and create waterlogging (for example soil sodicity, compaction) to be important, then can negatively impact plant growth. Therefore, we might also expect correlations between soil constraints and crop growth, particularly if surface/subsoil sodicity or compaction is present [2]. On the other hand, when in-season rainfall is reasonably consistent and sufficient for good crop growth, we might expect only limited impact of soil constraints on the spatial variation of yields.

Thus, the different patterns of spatial variation of yield (within fields) between wet and dry years might be related to the spatial variation of soil constraints. Based on this assumption, it should be possible to detect soil constraints from yield collected over many growing seasons. However, the availability of long-term archives of yield monitor data is limited. Therefore, this study used remote-sensing data to represent crop growth by extracting a vegetation index (average NDVI) [7] from a series of imageries around peak biomass. The NDVI will not directly represent yield, yet it is useful to produce vegetation indices from vegetation greenness and density [8–12]. This index has been used in previous work [13–15] and showed a reasonable correlation with crop yields in the study region. As a result, when the index is compared with soil constraints, it might be able to detect different impacts of soil constraints in different rainfall years.

Accordingly, this study aimed to analyze how NDVI assesses the spatial variation of soil constraints under different rainfall conditions. The research questions are:

- How does the spatial pattern of the average NDVI within fields differ between years, and is it related to rainfall?
- Compared to actual yield, how does the average NDVI explain the soil constraints?
- Does the pattern of average NDVI in dry and wet years explain the soil constraints?

2 Material and Methods

2.1 Study Area

The study area involved five fields located in Australia's northern grain-growing region (as defined by the Grains Research and Development Corporation of Australia, GRDC), which is dominated by winter grains cropping. The region has a semi-arid climate, with 500–800 mm annual rainfall, mainly during the summer months. We focussed on these five fields for which soil data and yield monitor data were compiled in earlier work [16–20] (Fig. 1).

2.2 Datasets and Pre-processing

2.2.1 Satellite and Rainfall Data

This work used 30-m pixel resolution satellite imageries from Landsat-5 Thematic Mapper (TM), Landsat-7 Enhanced Thematic Mapper Plus (ETM+), and Landsat-8 Operational Land Imager (OLI) collected between 1999 to 2019. Standardized surface reflectance was derived according to Flood et al. (2013) [21], and cloud and cloud-shadow were masked from images using the Fmask algorithm [22]. The six bands of each satellite

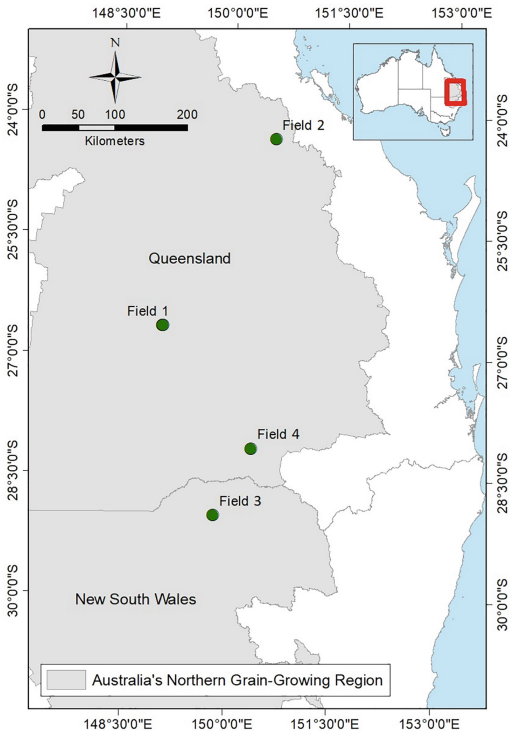

Fig. 1. The study area in Australia's Northern grain-growing region, and the five fields considered in this analysis.

were used, representing the blue, green, red, near-infrared, and two shortwave infrared portions of the electromagnetic spectrum. Some imageries were incomplete due to partial cloud coverage or the 'SLC-off' issue with Landsat 7. Only images with at least 75% coverage of each yield map's pixels were included. For incomplete images but had ≥75% coverage, gaps were filled by regression kriging as follows. First, the image (from the same season as the incomplete image) with the highest correlation with the incomplete image was selected as the covariate (provided it covered the missing pixels). Then a linear model was fitted to predict the missing pixels before the residuals from this linear model were kriged and added to the linear function to give the fill values. Furthermore, these images were used to create average NDVI (Normalized Difference Vegetation Index) to represent the yield index.

Besides, daily rainfall data was extracted from the 5-km gridded dataset, obtained from SILO (Scientific Information for Land Owners), a database of Australian climate data (https://www.longpaddock.qld.gov.au/silo/).

2.2.2 Soil Constraint Data

This research assumed that the soil constraints were temporally stable throughout the period (1999–2019). Thus in this research, we used a set of soil constraint measurements

compiled in earlier work, in which eight to twelve soil profiles were sampled per field between April and May 2009 [16–19]. The sampled profiles were split into eight depth with midpoints 0.05, 0.2, 0.4, 0.6, 0.8, 1, 1.2 and 1.4 m. The samples were dried at 400 °C in a forced-draught oven and ground to pass through a <2-mm sieve [19]. Among a suite of soil properties that were measured, we focused on four that were indicative of particular soil constraints: ESP (Exchangeable Sodium Percentage), ECse (electrical conductivity of a solution extracted), Cl (Chloride) concentration, and EMgP (Exchangeable Magnesium Percentage). ECse and Cl content were assessed for all eight depths, while ESP and EMgP were assessed for four depths; 0.05, 0.4, 0.8 and 1.2 m. Cl content and ECse were determined in 1:5 soil:water suspension, while ESP was calculated from Na ration to CEC, determined using 1_M NH_4Cl extracting solution [23].

2.3 Initial Data Processing Methods

2.3.1 Detecting Years to Be Included in the Analysis

This analysis included remote-sensing data from 1999 to 2019. However, it would not be appropriate to include in the analysis (with respect to soil constraints) the remote-sensing data from all years; for some years, a crop might not have been sown (in very dry years, it is common for growers to decide not to plant crops to avoid crop failure), while for other years the remote-sensing data might be insufficient to provide a confident spatial representation of crop growth and yield. Since our aim was to provide a means of analysis based on the remote-sensing data, we defined a series of heuristics to detect the years to be included in the pursuing analysis. For each field, we extracted the field-median NDVI from all the imageries in a certain year and checked that (i) there were at least five imageries in a certain year, (ii) maximum field-median NDVI in a year was more than 0.3, (iii) maximum field-median NDVI was between mid-June until end of October, (iv) field-median NDVI of the beginning and the end of the growing season were at least half of the maximum field-median NDVI, and (v) the growing season had at least 120 days interval. In addition to these heuristics, we inspected the imagery for evidence of spatially differential management and excluded any seasons where such evidence was found. We only used data from fields that were managed in a spatially uniform way so that spatial differences in crop growth would not be due to differential management, but predominantly the effects of soil variability.

2.3.2 Selecting Suitable Imageries

From the previous research, several well-known vegetation indices such as NDVI, RVI, EVI, and EVI2 taken from around the time of their peak showed a good prediction of yield patterns for wheat crops in eastern Australia. Therefore, this study used one of those indices, NDVI, averaged over a window from 64 days before until 64 days after the peak NDVI. Furthermore, we filtered this series of images by only including those for which the field-median NDVI was at least 60% of the peak of the field-median NDVI. From these filtered images, we calculated their average, which we refer to from hereon as the average NDVI for each year.

2.3.3 In-Crop Rainfall Determination

In this work, 5 km grided daily rainfall from the Australian climate database, SILO (Scientific Information for Land Owners), was extracted into tabular daily rainfall. We calculated in-crop rainfall from this rainfall data, which was defined as cumulative rainfall from 3.5 months before to 1.5 months after peak NDVI. We assumed that the rainfall during this period would be the most crucial rainfall influencing yields or crop productivities and that the impact of soil constraints on the spatial variation of yield would be dependent on this in-crop rainfall. The cumulative rainfall of each year was further classified into three different classes: low, medium, and high representing dry years, medium rainfall years, and wet years, respectively. The years with in-crop rainfall under 100 mm were classified as dry years, 100–150 mm were classified as medium rainfall years, and more than 150 mm were classified as wet years.

2.4 Statistical Analysis Methods

2.4.1 Assessing Average NDVI Similarity Within a Certain Rainfall Year

The first analysis in this work was to test whether there was evidence of distinct patterns of spatial variation of the average NDVI for years in a certain rainfall class — for instance, do maps of the average NDVI for dry years look more similar than maps from moderate rainfall years? The analysis was conducted by calculating the average correlation between pairs of yield-index maps in each rainfall category. Significance of the difference in average correlation was determined by randomly re-assigning rainfall classifications to the maps and recalculating the difference in average correlation (the test statistic) to generate a distribution of this test statistic under the null hypothesis (no difference between the average correlations). We compare the average correlations of dry years with those of medium rainfall years and those of wet years with medium rainfall years to investigate whether there is evidence in the remote-sensing data of more distinct patterns of spatial variation in the more extreme rainfall years.

2.4.2 Assessing Yield and Soil Constraints Correlation in Different Rainfall Years

Before undertaking analysis using remote-sensing data from all years (1999–2019), we first checked whether analysis based on the average NDVI would give similar results to analysis based on yield monitor data, using just the subset of years for which yield monitor data were collected. This analysis compared the soil constraints with the monitored yield data and with the average NDVI. The yield monitored data and the average NDVI were extracted for each soil sample point and for each yield-monitored year. Then we calculated the average yield for each spatial point (averaged over all monitored seasons) based on the available monitored data and calculated correlations with the soil constraints (for each field, each soil constraint, and each sampled soil depth); we did the same thing with the average NDVI in place of the yield monitor data. A similarity of results from these two different analyses would indicate that the average NDVI is providing a useful surrogate for yield in the context of spatial diagnosis of soil constraints.

This work used data from eight to twelve sampled soil profiles in each field to assess soil constraints and their relationships with the average NDVI in different rainfall years.

Following validation of the approach, we applied the method with the remote-sensing data from all cropped years, splitting those years into dry, moderate, and wet years according to in-crop rainfall.

3 Result and Discussion

3.1 Cropped Years for Each Field

The study area involved four fields located in Australia's northern grains-growing regions, which is dominated by winter grains cropping (Table 1).

Table 1. Cropped years

Fields	Cropped Years
Field 1	1999, 2001, 2002, 2003, 2004, 2005, 2006, 2007, 2008, 2009, 2010, 2011, 2013, 2014, 2015, 2016, 2017, 2018, 2019
Field 2	1999, 2002, 2003, 2004, 2005, 2006, 2007, 2009, 2010, 2013, 2014, 2015, 2017
Field 3	1999, 2000, 2002, 2003, 2006, 2007, 2009, 2012, 2013, 2017
Field 4	2000, 2001, 2002, 2003, 2004, 2005, 2006, 2008, 2009, 2010, 2011, 2012, 2013, 2014, 2015, 2016, 2017

Table 2. In-crop rainfall classification

Fields	Dry Years	Medium Rainfall Years	Wet Years
Field 1	1999, 2002, 2006, 2017, 2018, 2019	2001, 2004, 2009, 2013, 2014, 2015	2003, 2005, 2007, 2008, 2010, 2011, 2016
Field 2	2002, 2013, 2014, 2017	1999, 2003, 2004, 2006, 2007, 2009	2005, 2010, 2015
Field 3	2009, 2013, 2017	1999, 2000, 2006	2002, 2003, 2007, 2012
Field 4	2000, 2002, 2013	2004, 2006, 2009, 2011, 2014, 2017	2001, 2003, 2005, 2008, 2010, 2012, 2015, 2016

Table 3. Mean correlation between two years in the same in-crop class. (*significant correlation)

Fields	Mean Correlation			p-value	
	Dry	Medium Rainfall	Wet	Dry > Medium	Wet > Medium
Field 1	0.62	0.54	0.45	0.03*	NA
Field 2	0.69	0.65	0.28	0.35	NA
Field 3	0.94	0.75	0.97	0.25	<0.01*
Field 4	0.60	0.34	0.34	0.26	NA

3.2 In-Crop Rainfall

Table 2 shows the cropped years that were classified into each rainfall class according to in-crop rainfall. Over all fields, at least three years fell into each in-crop rainfall category, which provided enough data to allow some statistical analysis of differences between the categories.

3.3 Average NDVI Spatial Pattern in Different Rainfall Years

We calculated the mean correlation between average NDVI maps for different years in each in-crop rainfall category (Table 3). All fields had a higher correlation in dry years than in medium rainfall years, although it was only significantly higher for Field 1. (Note that fields with fewer cropped years are less likely to show significant differences between correlations than fields with more cropped years.) This finding suggests that although there might in general be some more distinctive patterns of spatial variation in dry years than in wet years, the evidence for individual fields was only significant for one of the four fields. Average NDVI maps for one of the four fields showed a higher correlation in wet years compared to medium rainfall years, with that for Field 3 being significantly higher.

A more distinctive pattern of variation for the average NDVI suggests a common driver of variation in that subset of years. These results, therefore, suggest that the average NDVI for Field 1 in dry years and that for Field 3 in wet years are good candidates for variation that is related to soil constraints.

Average NDVI maps for Field 3 are shown in Fig. 2, for dry in-crop rainfall years (Fig. 2a), medium rainfall years (Fig. 2b), and wet years (Fig. 2c). The figure shows similar patterns in dry and wet year maps compared with the patterns in medium rainfall years; this visual assessment agrees with the statistical assessment (Table 3), which deemed the correlations of maps in wet years and in dry years to be greater than that in medium rainfall years (with significance for the wet-medium comparison). It shows that the area with a low yield is generally similar during the dry and wet years. But in the medium rainfall years, the area with low yield differed more between years (although this was largely due to the different pattern of the average NDVI in 2006).

3.4 Average NDVI Representativity to Replace Actual Yield Data

Before using the extracted NDVI from all cropped years for the full analysis, we examined whether analysis based on the NDVI would give similar results to that based on actual yield data. The correlations between monitored yield and soil constraints were calculated and compared with those based on the average NDVI from the same years. Figure 3 depicts the magnitude (size and darkness of circle) and sign (blue for positive and red for negative) of correlations, only showing those that were significant ($p < 0.05$), which demonstrates that results from both analyses were quite similar. Both actual yield and NDVI showed significant correlations with Cl content and ECse at Field 3 and Field 4 and ESP at Field 3. This result indicates that extracted NDVI in this work could provide a useful surrogate for monitored yield data in the diagnosis of soil constraints impacting crop yields.

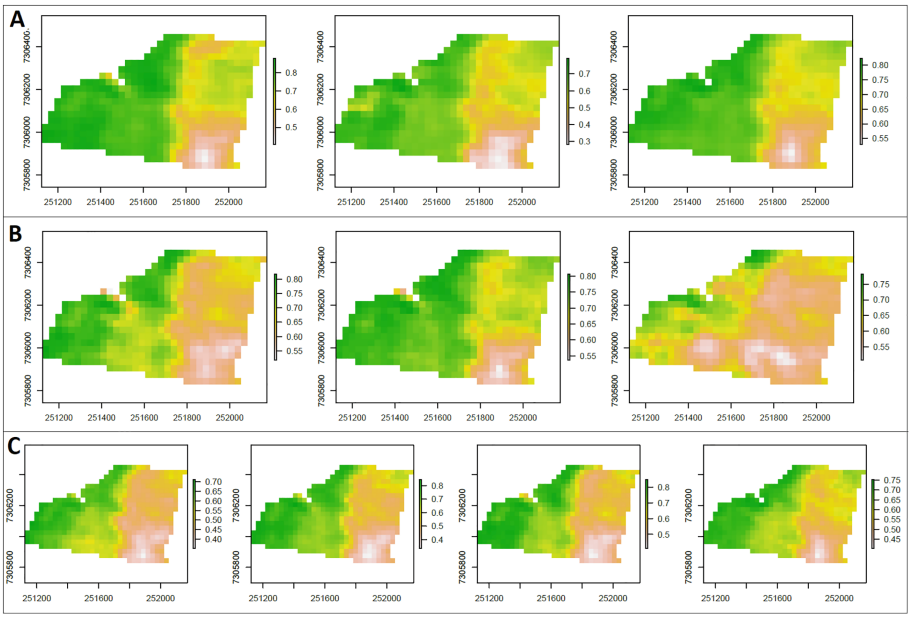

Fig. 2. Average NDVI during dry years (a), medium rainfall years (b), and wet years (c).

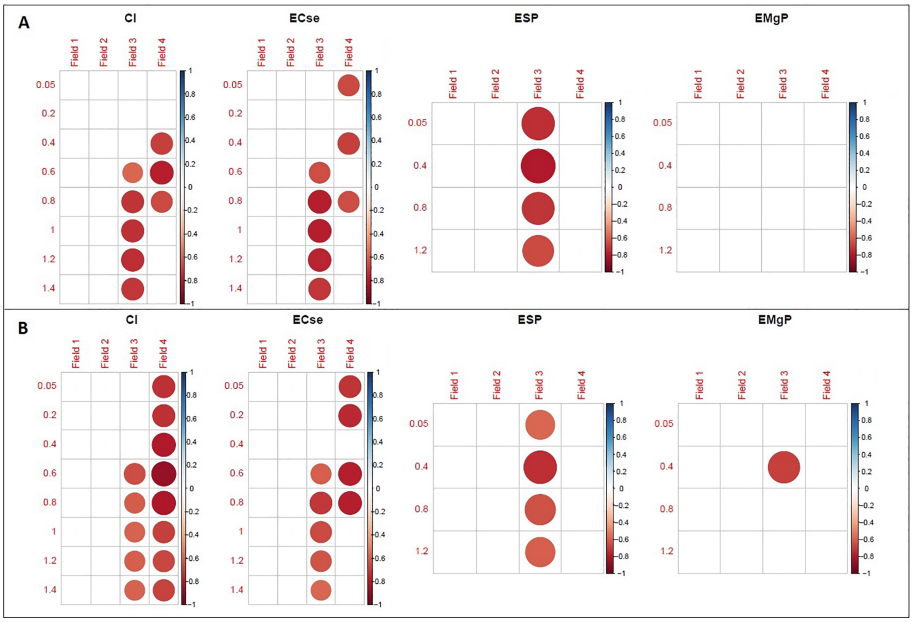

Fig. 3. Correlation plot of actual yield and constraint parameters (a), of average NDVI and constraint parameters (b) in different profile depth. The darker and the bigger the points, the higher the correlations.

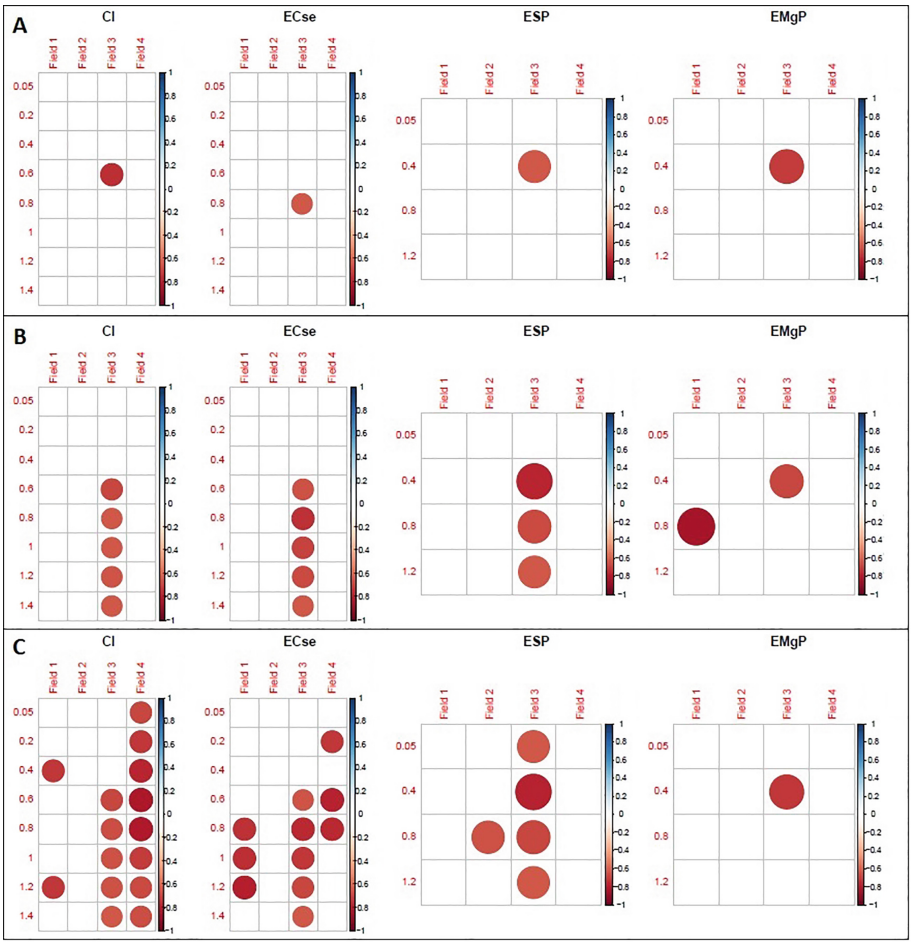

Fig. 4. Correlation plot of average NDVI and constraint parameters in dry (a), medium rainfall (b), and wet years (c) in different profile depths. The darker and the bigger the points, the higher the correlations.

3.5 Average NDVI Correlation to Soil Constraints in Different Rainfall Years

Theoretically, the importance of the soil's capacity to supply the crop with water is more important in dry compared with medium rainfall or wet years. A soil constraint impacting PAW might be expected to have greater impact in dry years, and so spatial variation in the soil constraint might correlate strongest with spatial variation in yield from dry years. However, Fig. 4 shows that there were more significant correlations between yield and the presence of constraints in the years with high in-crop rainfall. One of the possible reasons for this that high rainfall is causing soil waterlogging, which is a known problem in soils affected by sodicity.

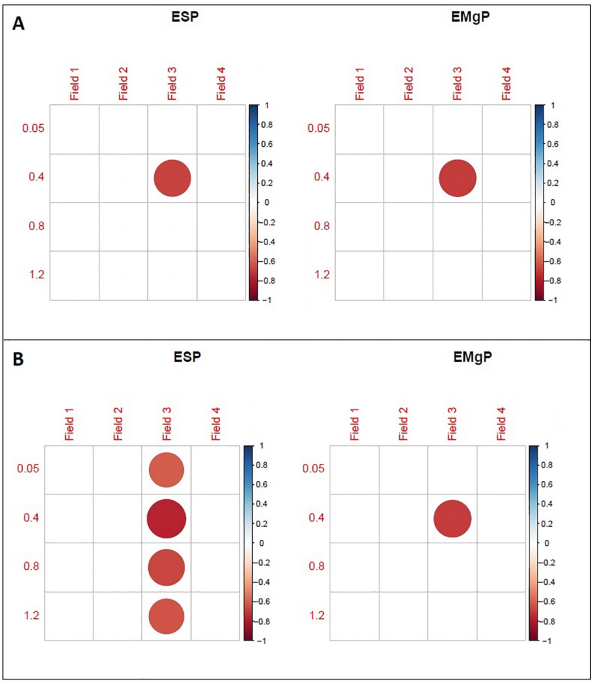

Fig. 5. Correlation plots of average NDVI and constraint parameters on years without waterlogging event (a) and years with waterlogging events (b).

3.6 Average NDVI Correlation to Soil Constraints in Different Waterlogging Events

As noted, one possible explanation for stronger correlations between NDVI and soil constraints in wet years is that certain constraints are triggered by waterlogging events; an example would be soil sodicity, which can increase the crusting after intense rainfall events (Table 4). To investigate the plausibility of this, we defined a potential waterlogging event as a period of seven days' cumulative rainfall of more than 50 mm; years were classified as those with no such waterlogging events and years with waterlogging events. Although the correlations in the years with at least one waterlogging event is significant, results are generally similar to those from the analysis for wet years (Fig. 5), and thus do not provide a strong indication that this is the reason behind the strong correlations found in wet years.

Table 4. Waterlogging Events

Fields	No waterlogging events	Waterlogging events
Field 1	1999, 2006, 2009, 2011, 2013, 2017, 2018, 2019	2001, 2002, 2003, 2004, 2005, 2007, 2008, 2010, 2014, 2015, 2016
Field 2	1999, 2003, 2006, 2007, 2009, 2013, 2014, 2015, 2017	2002, 2004, 2005, 2010
Field 3	1999, 2000, 2009, 2012, 2013	2002, 2003, 2006, 2007, 2017
Field 4	2000, 2002, 2004, 2006, 2011, 2013, 2014, 2016, 2017	2001, 2003, 2005, 2008, 2009, 2010, 2012, 2015

4 Conclusion

This work investigated the potential of remote-sensing imagery for diagnosing the impacts of soil constraints in different rainfall years. The results showed that the yield index during wet years, in general, showed stronger correlations with soil constraints. One possible interpretation is that the stronger correlations in wet years are due to waterlogging events triggering crusting and reducing water infiltration, for instance in areas impacted by soil sodicity. The analysis of data separated by years with potential waterlogging events showed that the average NDVI during water-logged years better assessed the soil constraint than those without waterlogging events but did not provide compelling evidence for this explanation over the separation into wet, moderate, and dry rainfall years. Alternatively, it could be that the imageries selected to calculate the average NDVI (those within 64 days of the peak field-median NDVI, and with a field-median NDVI greater than 60% of its peak value) were not a good representation of yield; another possibility is that the period of rainfall (3.5 months before peak NDVI to 1.5 months after peak NDVI) used was not the most appropriate for the analysis; further analysis of this will be looked at in future.

Acknowledgments. This research was supported and funded by the Grains Research and Development Corporation (GRDC) of Australia under project number UOQ1803-003RTX. Landsat imagery is provided by the United States Geological Survey, and the support and resources provided by the Queensland Remote Sensing Centre, Department of Environment and Science, and the help of Matt Pringle, is gratefully acknowledged. The authors also thank for helpful discussions from Scott Chapman.

Authors' Contributions. Conceptualization: Fathiyya Ulfa, Thomas G. Orton, Yash P. Dang, Neal W. Menzies; Methodology: Fahiyya Ulfa, Thomas G. Orton; Analysis and result interpretation: Fathiyya Ulfa, Thomas G. Orton; Writing - original draft preparation: Fathiyya Ulfa; Writing - review and editing: Thomas G. Orton, Yash P. Dang, Neal W. Menzies. All authors have read and agreed to the published version of the manuscript.

References

1. SalCon, "Salinity Management Handbook." Queensland Departement of Natural Resources and Mines, Indooroopilly, Qld, 1997.
2. R. R. Weil and N. C. Brady, *The Nature and Properties of Soils, Global Edition*, 15th ed. Pearson Education Limited, 2017.
3. N. Hussain, F. Mujeeb, G. Sarwar, H. G., and M. K. Ullah, "Soil salinity / sodicity and ground water quality changes in relation to rainfall and reclamation activities," *IWMI Books, Reports*, 2002.
4. D. Isidoro and S R Grattan, "Predicting soil salinity in response to different irrigation practices, soil types and rainfall scenarios," *Irrig. Sci.*, vol. 29, pp. 197–211, 2011.
5. K. L. Page *et al.*, "Management of the major chemical soil constraints affecting yields in the grain growing region of Queensland and New South Wales, Australia – a review," *Soil Res.*, vol. 56, no. 8, p. 765, Dec. 2018.
6. C. Tang, Z. Rengel, E. Diatloff, and C. Gazey, "Responses of wheat and barley to liming on a sandy soil with subsoil acidity," *F. Crop. Res.*, vol. 80, no. 3, pp. 235–244, 2003.
7. C. J. Tucker, "Red and photographic infrared linear combinations for monitoring vegetation," *Remote Sens. Environ.*, vol. 8, pp. 127–150, 1979.
8. T. Bai, N. Zhang, B. Mercatoris, and Y. Chen, "Jujube yield prediction method combining Landsat 8 vegetation index and the phenological length," *Comput. Electron. Agric.*, vol. 162, pp. 1011–1027, 2019.
9. A. W. Goodwin, L. E. Lindsey, S. K. Harrison, and P. A. Paul, "Estimating wheat yield with normalized difference vegetation index and fractional green canopy cover," *Crop. Forage Turfgrass Manag.*, vol. 4, no. 1, Jul. 2018.
10. N. Kobayashi, H. Tani, X. Wang, and R. Sonobe, "Crop classification using spectral indices derived from Sentinel-2A imagery," *J. Inf. Telecommun.*, vol. 4, no. 1, pp. 67–90, Nov. 2020.
11. Y. R. Lai, M. J. Pringle, P. M. Kopittke, N. W. Menzies, T. G. Orton, and Y. P. Dang, "An empirical model for prediction of wheat yield, using time-integrated Landsat NDVI," *Int. J. Appl. Earth Obs. Geoinf.*, vol. 72, pp. 99–108, 2018.
12. J. Yeom *et al.*, "Comparison of vegetation indices derived from UAV data for differentiation of tillage effects in agriculture," *Remote Sens.*, vol. 11, no. 13, 2019.
13. F. Ulfa, T. G. Orton, Y. P. Dang, and N. W. Menzies, "A comparison of remote-sensing vegetation indices for assessing within-field variation of wheat yield," in *Proceeding of the 20th Agronomy Conference*, 2022.
14. F. Ulfa, T. G. Orton, Y. P. Dang, and N. W. Menzies, "Developing and Testing Remote-Sensing Indices to Represent within-Field Variation of Wheat Yields: Assessment of the Variation Explained by Simple Models," *Agronomy*, vol. 12, no. 2, 2022.
15. F. Ulfa, T. G. Orton, Y. P. Dang, and N. W. Menzies, "Are Climate-Dependent Impacts of Soil Constraints on Crop Growth Evident in Remote-Sensing Data?," *Remote Sens.*, vol. 14, no. 21, p. 5401, 2022.
16. Y. P. Dang *et al.*, "Electromagnetic induction sensing of soil identifies constraints to the crop yields of north-eastern Australia," *Soil Res.*, vol. 49, no. 7, pp. 559–571, 2011.
17. Y. P. Dang, M. J. Pringle, M. Schmidt, R. C. Dalal, and A. Apan, "Identifying the spatial variability of soil constraints using multi-year remote sensing," *F. Crop. Res.*, vol. 123, pp. 248–258, 2011.
18. Y. P. Dang *et al.*, "High subsoil chloride concentrations reduce soil water extraction and crop yield on Vertosols in north-eastern Australia," *Aust. J. Agric. Res.*, vol. 59, no. 4, p. 321, Apr. 2008.
19. Y. P. Dang *et al.*, "Diagnosis, extent, impacts, and management of subsoil constraints in the northern grains cropping region of Australia," *Aust. J. Soil Res.*, vol. 48, pp. 105–119, 2010.

20. Y. P. Dang and P. W. Moody, "Quantifying the costs of soil constraints to Australian agriculture: a case study of wheat in north-eastern Australia," *Soil Res.*, vol. 54, pp. 700–707, 2016.
21. N. Flood, T. Danaher, T. Gill, and S. Gillingham, "An operational scheme for deriving standardised surface reflectance from landsat TM/ETM+ and SPOT HRG imagery for eastern Australia," *Remote Sens.*, vol. 5, no. 1, pp. 83–109, 2013.
22. Z. Zhu, S. Wang, and C. E. Woodcock, "Improvement and expansion of the Fmask algorithm: cloud, cloud shadow, and snow detection for Landsats 4-7, 8, and Sentinel 2 images," *Remote Sens. Environ.*, vol. 159, pp. 269–277, 2015.
23. G. E. Rayment and F. R. Higginson, *Australian Laboratory Handbook of Soil and Water Chemical Methods*. Melbourne, Vic.: Inkata Press, 1992.